Astron. Astrophys. 342, 773–784 (1999)

ASTRONOMY AND ASTROPHYSICS

# Dust extinction and intrinsic SEDs of carbon-rich stars

## II. The hot carbon stars⋆,⋆⋆,⋆⋆⋆

**J. Bergeat, A. Knapik, and B. Rutily**

Centre de Recherche Astronomique de Lyon (UMR 5574 du CNRS), Observatoire de Lyon, 9 avenue Charles André, F-69561 St-Genis-Laval Cedex, France

Received 6 August 1998 / Accepted 24 November 1998

**Abstract.** The present work is an extension of a recent study by Knapik & Bergeat (1997, henceforth called Paper I) of the spectral energy distributions (SEDs) of about 300 cool carbon-rich variables and of the interstellar extinction observed on their line of sights. The methods were originally developed for Semi-Regular (SR) and Irregular (L)-variables. Shortly, this is a kind of a pair method making use simultaneously of the whole SED from UV to IR.

Our approach is applied here to the galactic carbon-rich giants with bluer SEDs, namely the hot carbon (HC) stars, including many "constant" stars and a minority of variables: AC Her a RV Tau star, the R Coronae Borealis (RCB) stars and others. Some HdC (i.e. carbon-rich hydrogen deficient stars) and Ba II stars are also considered. The total number of studied HC stars amounts to about 140. With few exceptions, the colour excesses for interstellar extinction are found in good agreement with the field values from maps published in the literature, taking into account the approximate distances to our stars from HIPPARCOS data (1997, henceforth called ESA) or binarity. We propose a classification scheme with six photometric groups (or boxes: HC0 to HC5) from the bluest to the reddest SEDs. Oxygen-rich SEDs earlier than HC0, are attributed to the hottest stars (AC Her, most RCB-variables and a few others). Previous findings are confirmed of a junction between oxygen-rich and carbon-rich SEDs at spectral type G. The latest (HC5) group is immediately close to the earliest one in Paper I, namely CV1. The sequence of groups then goes regularly from HC0 to CV6.

Substantial infrared excesses with respect to our solutions are found in HD 100764 a HC1 carbon star, AC Her a G0g RV Tau star, and the RCB stars classified in either HC or oxygen-groups. The colour excesses at maximum light can usually be attributed to interstellar reddening, with neutral circumstellar (CS) reddening (large grains) or no CS extinction at all on the line of sight (non spherical geometry) as possible explanations. The latter model (disc or patchy distribution through successive puffs) is favoured. Two RCB variables for which we exploit SEDs on a rising branch (V CrA) or minimum light (RS Tel), show CS laws, respectively a selective extinction compatible with small grains and an extinction partly neutral indicative of large grains on the line of sight.

**Key words:** stars: carbon – stars: circumstellar matter – stars: AGB and post-AGB – ISM: dust, extinction

### 1. Introduction

Knapik & Bergeat proposed in Paper I, the first classification of the carbon variables in discrete photometric groups, independently of any spectral classification. The method was validated through colour-colour and colour-galactic latitude diagrams. It provides for every star sufficiently documented, a carbon variable group CVi (intrinsic SEDs from i = 1 the early one to i = 6 the late one) and the value of the interstellar extinction $\mathrm{A_J}$ in the J-filter. The colour excess is $\mathrm{E\,(B-V)} \simeq 1.15\mathrm{A_J}$ for the mean extinction law of the diffuse interstellar medium (Mathis 1990) which was shown to be appropriate. A good agreement was obtained in most cases between those colour excesses and the field values from maps found in the literature. No gap was actually observed and discrete CVi-groups are adopted here only for convenience. The main features of this new pair method are

- the simultaneous use of the whole spectral range from UV to IR (up to 17 wavelengths with equal weights *a priori*),
- the derivation of an accurate linear fit of the calculated $\mathrm{y}\,(\lambda)$ quantity as defined in Sect. 2.2., vs. the adopted reddening law $\mathrm{r}\,(\lambda)$ (see Figs. 1, 3, 6, 7, 8, and 9),
- $\mathrm{E\,(B-V)} \simeq 0.02$–$0.03$ as a detection threshold,
- the derivation of a k-factor (Eq. (7) in Paper I), which should be a squared angular diameter on a relative scale (and not an angular diameter as erroneously stated in Sect. 6 of Paper I).

The quantity $\mathrm{k}^{1/2}$ showed the correlation with true parallaxes from ESA expected for stars populating a given range in linear diameters (see Fig. 3 and Sect. 6 of Knapik et al. 1998). We must emphasize that photometric classifications do not correlate

*Send offprint requests to*: J. Bergeat

⋆ This research has made use of the Simbad database operated at CDS, Strasbourg, France.

⋆⋆ Partially based on data from the ESA HIPPARCOS astrometry satellite

⋆⋆⋆ Tables 3 and 4 are only available in electronic form at the CDS via anonymous ftp 130.79.128.5

well with the spectroscopic classification of carbon stars (Shane 1928, Keenan & Morgan 1941, Keenan 1993; see Paper I). This missing correlation between photometry and spectroscopy was a strong motivation for our study. The case is completely different for oxygen-rich stars, and we were able to make use of averaged indices compiled from the literature (Johnson 1966, Johnson et al. 1968, Bessell 1979, Bessell & Brett 1988, and Koornneef 1983) in our analysis of Ba II stars (Bergeat & Knapik 1997). The obtained SEDs were named according to the corresponding spectral type and luminosity class (d for class V dwarfs, g for class III giants and sg for class Ib supergiants, e.g. G2d, G8g or M2sg). The same notation is kept hereafter whenever oxygen-type SEDs are considered.

The study in Paper I was concentrated on carbon stars with small amplitudes of variations (namely Lb or SR variables) making use of the six CVi-groups. Here we propose an extension of our work to the hotter carbon stars with bluer SEDs and to related stars. The HC stars, either variables or non-variables (the latter being a majority), are studied in Sect. 2. Six intrinsic mean SEDs we named HC0 (the earliest one) to HC5 (the latest one, close to CV1) are adopted. A few stars classified in Stephenson (1989) or usually considered as close to carbon stars (RCB variables, a few Ba II or CH or HdC stars..) do exhibit SEDs better fitted by oxygen-types SEDs (Sect. 3). Contrary to the variables of Paper I which presumably are all bright stars located on the asymptotic giant branch (AGB), many stars studied here are much fainter and possibly closer to the red giant branch (RGB). Some of them (e.g. the RCB variables) are luminous stars (bright giants or supergiants) usually considered as AGB or post-AGB objects. The cases of CS extinction and emission is discussed whenever possible, and a few conclusions are reached.

Every studied star was searched for variability in Kholopov et al. (1985, henceforth called GCVS) and the subsequent lists published in the Inf. Bull. on Var. Stars (67th to 73rd). Some of them were found in the New Catalogue of Suspected Variable Stars (Kukarkin et al. 1982, henceforth called NSV) which were not included in the GCVS as yet. They are denoted by NSV followed by the corresponding entry. Accurate HIPPARCOS photometry (ESA) was also considered when available. The remaining stars, presumably "constant" to the present accuracy, are usually named from their entries in the HD or BD catalogue.

## 2. The hot carbon stars

### *2.1. The sample of unreddened HC stars*

First of all, we intend to identify unreddened objects among a sample of about 140 documented HC stars. They exhibit SEDs earlier than the CV1-SED (the earliest SED in Paper I), i.e. bluer colour indices. Finding simultaneous observation sets or consistent non-simultaneous data was the main difficulty we met when dealing with variable stars of Paper I. Most stars considered here are non-variable to the present accuracy of measurements or variables of very small range (e.g. the Hp-data of ESA, vols.11–12). Easier analyses are thus expected. The opposite situation was actually observed since:

**Table 1.** A list of the fifty-one HC stars found unreddened in the present study. The stars entries in the C catalogue (Stephenson 1989) are given. By "unreddened", we mean a star with $\mathrm{E(B-V)} \leq 0.02$–$0.03$.

| HC1 | HC1 | HC2 | HC2 | HC3 | HC4 | HC5 |
|---|---|---|---|---|---|---|
| 102 | 3795 | 80 | 2919 | 256 | 92 | 327 |
| 1035 | 5227 | 135 | 3058 | 594 | 258 | 2404 |
| 2282 | 5549 | 196 | 3469 | 2428 | 357 | 2449 |
| 2383 | 5980 | 378 | 3735 | 3298 | 576 | 4873 |
| 2925 | | 2396 | 3912 | 3666 | 2626 | 5147 |
| 3066 | | 2829 | 4947 | 4972 | 2715 | |
| 3379 | | 2892 | 4978 | | 3319 | |
| 3586 | | 2900 | 5761 | | 3614 | |
| 3606 | | 2914 | 5937 | | 4485 | |

– less data was available on the average for every star,
– most earlier stars are intrinsically fainter than the previously studied ones, resulting in larger scatter in the observations,
– no colour index can be found as sufficiently constant on the HC-range and thus no colour-latitude diagrams could be used,
– no colour-colour diagram documented with sufficient accuracy (like $\mathrm{CI_B}$ = [0.78]-[1.08] vs. [1.08]-K-$\mathrm{CI_B}$ in Fig. 2 of Paper I, as adapted from Baumert 1972) could be found with a reddening vector nearly rectangular to a narrow intrinsic locus.

Fortunately, many of those stars are nearby objects with distances less than 900 pc, and with high galactic latitudes. Thus we were able to select 51 stars presumably unreddened (see Table 1), making use of the maps of interstellar extinction as published by FitzGerald (1968), Neckel & Klare (1980), and Burstein & Heiles (1982). The approach differs here from the analysis of the CV stars in Paper I where various diagrams were first used, and then consistency with field maps checked.

### *2.2. The classification scheme of HC stars*

To apply our pair method we split the sample of 51 unreddened star into six boxes or groups we name HC0 to HC5. The SEDs of two stars in the same box, should not differ significantly (outside errors) in a systematic way, throughout the entire spectral range. The seventeen photometric bands used range from U ($\lambda \simeq 0.36\,\mu\mathrm{m}$) to the second ([25]) IRAS band as adopted in Paper I. The sixteen intrinsic indices:

$$\mathrm{I_0}\,(\lambda) = \mathrm{m_0}\,(\lambda) - [1.08]_0 \qquad (1)$$

and dispersions were finally calculated for every HC-group. The process was achieved by trial and error. Two accumulations appear (18 stars for HC2 and 9 stars for HC4 in Table 1) which were helpful. Then, the intermediary SEDs were put into HC3 while those earlier than HC2 could be gathered in HC1. The SEDs later than HC4 could be clustered in a single (HC5) group just intermediary between HC4 and CV1. The sixth (and earliest) group (HC0) was finally added to attempt the study of 4 reddened stars (no unreddened SED available). It is poorly defined

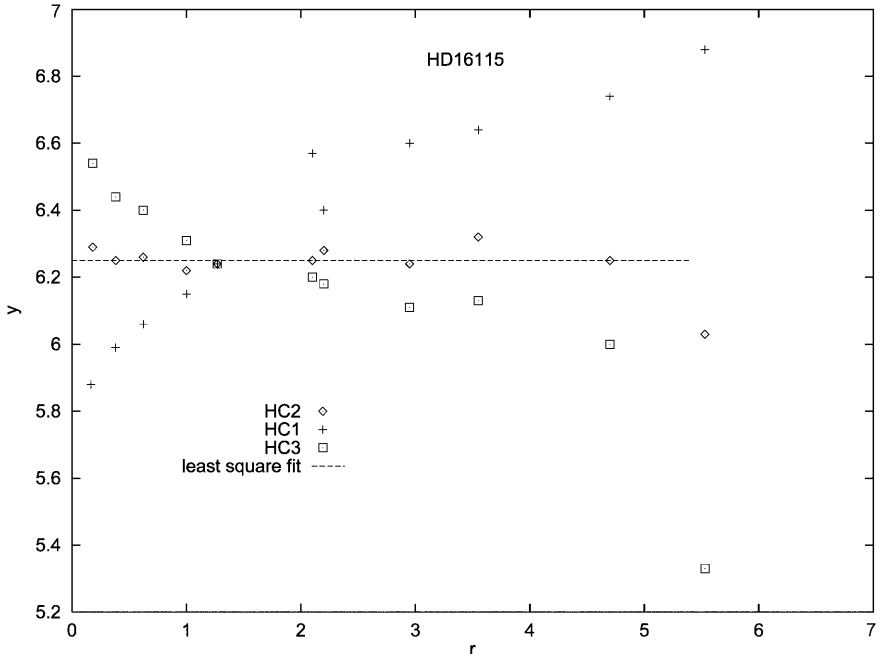


**Fig. 1.** The plot of y *vs.* r illustrating Eqs. (1) and (2) in the case of C378 = HD 16115 (HC2, E(B-V) = 0.0). The slope is $\mathrm{A(J)} \simeq 0.0$ the extinction at $\lambda = 1.25\,\mu\mathrm{m}$ and the intercept is $[1.08]_0 \simeq 6.25$ the dereddened magnitude at $1.08\,\mu\mathrm{m}$. See Sect. 2.2. for details.

**Table 2.** The six photometric groups (G) of the unreddened HC stars. The C-entry (Stephenson 1989) of a representative star is mentioned for each group (C4094 has actually $\mathrm{E(B-V)} = 0.05$). Three mean colour indices are given with their standard deviations. The closer oxygen-type SEDs "Ox" for giants (g) is quoted in the last column.

| G | C | B-V | $\mathrm{CI_B}$ | J-K | Ox |
|---|---|---|---|---|---|
| 0 | 4094 | $0.81 \pm 0.1$ : | $0.15 \pm 0.1$ : | $0.23 \pm 0.1$ : | G |
| 1 | 3606 | $1.13 \pm 0.07$ | $0.38 \pm 0.06$ | $0.46 \pm 0.08$ | K0 |
| 2 | 3469 | $1.30 \pm 0.08$ | $0.50 \pm 0.08$ | $0.77 \pm 0.07$ | K2 |
| 3 | 3298 | $1.36 \pm 0.16$ | $0.60 \pm 0.04$ | $0.87 \pm 0.1$ : | K3.5 |
| 4 | 576 | $1.72 \pm 0.14$ | $0.71 \pm 0.06$ | $0.97 \pm 0.10$ | K5 |
| 5 | 4873 | $1.79 \pm 0.18$ | $0.87 \pm 0.09$ | $1.21 \pm 0.08$ | M3 |

and the corresponding values of the indices are only tentative. Actually, the SEDs earlier than HC0 were classified as oxygen-rich ones (see Sect. 3) and the above four stars might be similar wrongly-classified objects. We are here at the junction between carbon-rich and oxygen-rich SEDs.

The main features of the six groups are shown in Table 2 where mean values of three colour indices ranging from blue to IR are given. They are bluer than their counterparts of the CV-groups for cool variables (see Table 1 of Paper I). The indices increase along the sequence HC0 to HC5 which is also the case along the sequence CV1 to CV6, with the exception of $\mathrm{CI_B}$ which remains close to 1.1 for CV1 to CV6, a remarkable property turned to advantage in Paper I. This is the reason why the transition between both categories was placed here (HC5-CV1) at an effective temperature of about 3300 K. The variability criterion did not prevail since about one-fourth of the HC stars are actually variables. As opposite to the case of CV stars, a correlation is observed with the spectral classification (R0 to R3 and C0 to C2 for HC3 and earlier groups; R4 and later and C3 or C4 for HC4 and HC5) but this is not a tight one.

### *2.3. The pair method applied to HC stars*

The method described in Sect. 4 of Paper I was then applied to the whole sample including reddened and unreddened stars as well. It makes use of the differences

$$\mathrm{y}\,(\lambda) = \mathrm{m}\,(\lambda) - \mathrm{I_0}\,(\lambda) \tag{2}$$

between the observed magnitudes

$$\mathrm{m}\,(\lambda) = \mathrm{m_0}\,(\lambda) + \mathrm{A}\,(\mathrm{J})\,\mathrm{r}\,(\lambda) \tag{3}$$

and, for a given group tentatively considered, the mean unreddened indices $\mathrm{I_0}\,(\lambda)$. If the latter are properly selected (i.e. if the appropriate HC-group is considered), a linear relation is thus expected between $\mathrm{y}\,(\lambda)$ and the adopted reddening law $\mathrm{r}\,(\lambda)$, the extinction $\mathrm{A}\,(\mathrm{J})$ at $\lambda_\mathrm{J}$ = 1.25 $\mu\mathrm{m}$ being the slope and $[1.08]_0$ = $\mathrm{m_0}\,(\lambda)$ - $\mathrm{I_0}\,(\lambda)$ the intercept. If the selected group and/or the adopted extinction law are wrong, the relation is no longer a linear one. The method is illustrated in Fig. 1 with the star C378 = HD 16115. It is shown to be HC2 with no appreciable reddening, i.e.

$$\mathrm{A}\,(\mathrm{J}) \simeq 0.01 \pm 0.01 \tag{4}$$

Strong curvatures are observed when the indices of HC1 or HC3 are used instead. The reader is referred to Paper I for full details, especially concerning the statistical analysis we apply. In the case of the $\left(^{13}\mathrm{C} - \mathrm{rich}\right)$ J-type star C378, no peculiarity was found, except for a slight excess in U (the extreme point on the right), a measurement which was ignored in the final statistics.

We have studied the 140 stars for grouping and extinction evaluation. The results are given in Tables 3 and 4 (only available in electronic form at the CDS), for 119 classical HC-stars and

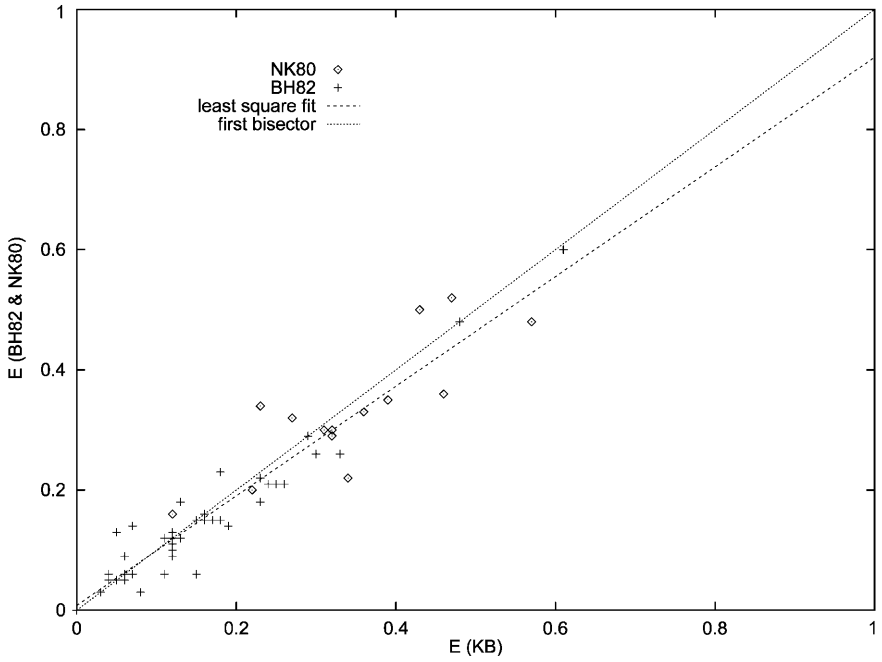


**Fig. 2.** A comparison of E(B-V) excesses from the maps and graphs of Neckel & Klare (1980, NK80) and Burstein & Heiles (1982, BH82) with values from the present paper (KB) for HC stars. The regression line (4) is also shown.

21 peculiar stars (including RCB variables, AC Her...). In Table 3, there are 17 variables from GCVS (14.3%), 12 suspected variables from NSV (10.1%) which makes 24.4% of variables and 75.6% (90 stars) of "constant" stars. The same format is used as in Table 3 of Paper I.

For oxygen-type SEDs, the indices $\mathrm{I}_0\,(\lambda)$ were taken with respect to V-magnitudes instead of $[1.08]_0$. This is the usual practice in the literature cited in Sect. 1. The intercepts of the linear fits in Figs. 6 to 9 are thus the dereddened values $\mathrm{V}_0$.

### *2.4. The obtained extinctions*

The intervals between two neighbouring HC-groups are larger in effective temperature than they are between the CV-groups. The preliminary calibrations yield 6000–3300 K and 3300–2000 K for the whole HC and CV ranges respectively. This is also illustrated by the range in "closer" oxygen-types as quoted in Table 2. The analysis of HC stars extinctions could then be less accurate than its counterpart for CV stars (Paper I). Our $\mathrm{E\,(B-V)}$ excesses are confronted in Fig. 2 to the field values extracted from the maps published in the literature. The correlation with FitzGerald (1968) is good but substantial scatter appears since the author provides only ranges. We show in Fig. 2 the comparison with the data of Neckel & Klare (1980) and Burstein & Heiles (1982). The linear fit found is:

$$\mathrm{E_{NK-BH}} = 0.912\,\mathrm{E_{KB}} + 0.008 \qquad (5)$$

with a correlation coefficient of only 0.902 (see Eq. 6 of Paper I for a definition). The standard deviation of the slope is 0.041 while it is 0.04 on a single ordinate estimate. The first bisector is thus at about two standard deviations from the above fit, which is not as good as the results of Paper I (which were within one standard deviation). The lower accuracy of the photometric data used here and the larger intervals in the HC-grid when compared to the CV-one, may be responsible for this situation. Finally, there is a marginal indication of an overestimate of about $9\%$ on the excesses determined for this sample, to be compared to $4\%$ or less in Paper I.

### *2.5. The case of C 3066 = HD 100764*

According to Mendoza (1968), some of the early R stars appear to have near IR excesses. Dominy et al. (1986) however found no excess in their infrared photometry of 31 early (R, CH, BaII) carbon stars. Having obtained extinction corrections for a sample of 119 classical HC stars (excluding RCB stars which are separately discussed in Sect. 3.), we checked the dereddened SEDs for such excesses against the mean intrinsic SED of the relevant HC-group. We ignore here a few (say 2 or 3) possible excesses as suggested by unconfirmed old data. Finally we are left with two stars (2 out of 126) namely C 4595 = HD 189605 (HC5, E(B-V)=0.16 with some excess from L') and C 3066 = HD 100764 (HC1, E(B-V)=0.0 with strong excesses starting from H). The former star has very strong excesses in the IRAS band-passes at 12 $\mu$m and 25 $\mu$m and is considered by Chan (1994) as a possible carbon star with IR silicate signature on the grounds of its low resolution IRAS spectrum (IRAS Science Team 1986, henceforth called LRS). The strength of the excesses we obtain (2.9 mag and 3.9 mag at 12 $\mu$m and 25 $\mu$m respectively) are in favour of this interpretation. This star will be discussed with other IR silicate CV carbon stars in a forthcoming paper.

The result E(B-V)=0.0 for HD 100764 is in excellent agreement with the published maps of interstellar extinction. The observed HIPPARCOS parallax is $(2.78 \pm 1.18)\mathrm{mas}$ i.e. a distance of $360^{625}_{250}\,\mathrm{pc}$ to sun. For V=8.84 we adopted, one obtains

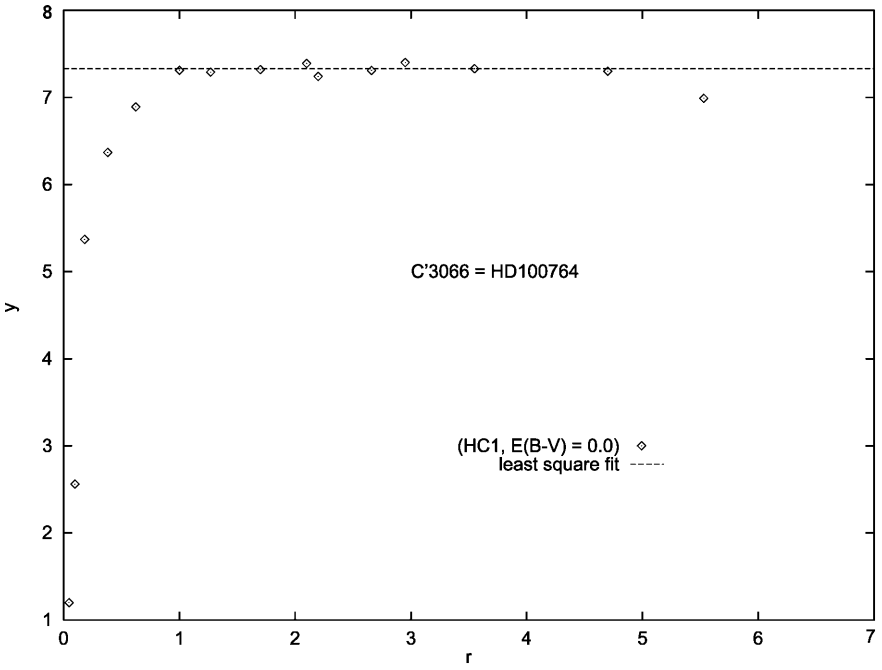


**Fig. 3.** Same as Fig. 1 for C 3066 = HD 100764: strong IR excesses are observed for $\mathrm{r} \leq 0.62$ (H-filter and beyond) when compared to the extrapolated dashed line (unreddened HC1).

$\mathrm{M_V} = 1.06^{-0.14}_{+1.83}$. Statistics on inaccurate observed parallaxes are moreover affected by biases (Knapik et al. 1998). The estimate of true parallax is 1.48 mas for a pseudo-star replacing HD 100764 in a corrected (de-biased) sample. We would then obtain $\mathrm{M_V} = -0.31$. The true value is lying probably between 1.06 and -0.31, since a statistical study by Vandervort (1958) showed that $\mathrm{M_V} = 0.44 \pm 0.29$ for R0-R2 stars, which is about halfway. This is also roughly consistent with 0.7 for K0 III stars. We study now in detail this latter star which is much earlier (HC1 against HC5, which corresponds to say 4700 K against 3500 K). This result is further confirmed by the (near IR) colour temperature Tc=4605 K and the CN-index of 29.8 (a measurement of the CN bands strengths in the red system) obtained by Baumert (1972), to be compared to the average values for the HC1-group, viz. $(4510 \pm 150)$ K and $25 \pm 10$.

This object is thus the only non-RCB HC1 star to be associated with a thick dust shell. Parthasarathy (1991) studied the spectral distribution of the IR excesses and attributed them to a spherical circumstellar dust shell. He concluded that this object might be similar to the carbon stars with IR silicate excesses (Little-Marenin 1986, Willems & de Jong 1986). There is however no silicate signature in the 8–13 $\mu$m spectrum obtained by Skinner (1994) which invalidates a possible connection. A slight emission near $11.5\,\mu\mathrm{m}$ attributable to SiC is possibly present. The faintness of this feature can be explained on the grounds of a large optical depth of the shell. Skinner's analysis was conducted in terms of either a spherical shell in which very large grains $\mathrm{a} \geq 0.5\,\mu\mathrm{m}$ of amorphous carbon are needed, or a disc (presumably pole on) with a distribution including small grains but peaked towards large grains ($\mathrm{a}^{-1}$ instead of $\mathrm{a}^{-3.5}$ for interstellar grains). The large grains were required to provide the large excesses observed in the IRAS range.

We show in Fig. 3 the result of our analysis of HD 100764. It is remarkable that $\mathrm{A\,(J)} = 0.00 \pm 0.01$, with practically no deviating point except for a slight excess in U (extreme right on the diagram) which is only marginally significant. The IR excesses start from the H-filter (extreme left in the diagram). The energy corresponding to this emission excess has to be compensated for by some absorption on the whole star spectrum. We emphasize here that our results rely upon the SED HC1, as deduced from 13 unreddened stars and confirmed through 19 reddened stars successfully analysed and classified HC1. We are left with two possible conclusions concerning the circumstellar extinction:

- it is essentially independent of wavelength at least up to $\lambda_\mathrm{J}$ = 1.25 $\mu$m which points to large grains (radii $\mathrm{a} \simeq 0.3\,\mu\mathrm{m}$ or even larger),
- and/or it is strongly non-spherical in distribution (e.g. a disc or torus seen at a large inclination angle nearly pole on) or even patchy.

The former hypothesis requires the optical depth in both absorption and scattering to be a constant within a few percents according to our results. This is not very likely although not impossible in principle. Large carbonaceous grains would then be expected, and substantial scattering due to large albedos might occur. High angular resolution in the visible range may help in establishing whether blurred images are indeed present. The latter possibility seems more likely, but constraints are raised by the data at hand. Let us assume that no extinction is present on the line of sight. We subtract our HC1-model extrapolated on the whole spectral range, thus obtaining the spectrum of the dust shell (see Fig. 4). Clearly, a wide distribution in dust temperatures is observed from an inner 900–1300 K to outer values less than 200–300 K (the true values depend on the nature and size of grains).

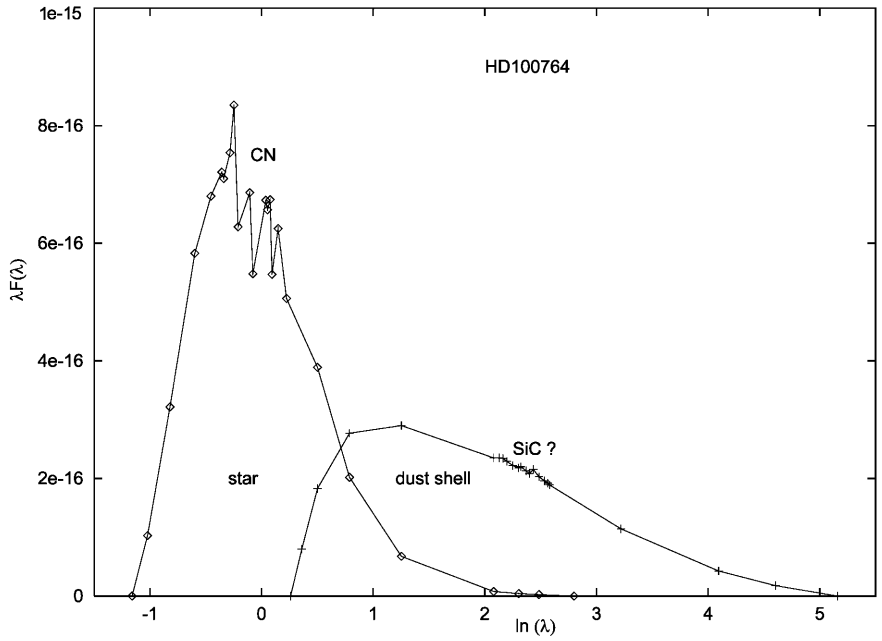


**Fig. 4.** The diagram of radiated powers for the HD 100764 star and shell (see Sect. 2.4.). Beyond $1.25\ \mu\mathrm{m}$, the star curve is an extrapolation of our model.

The coordinates adopted in Fig. 4 make the areas proportional to the integrated fluxes which gives $\mathrm{F}* = 4.88\mathrm{x}10^{-11}\mathrm{Wm}^{-2}$ and $\mathrm{F_{sh}} = 3.67\mathrm{x}10^{-11}\mathrm{Wm}^{-2}$, i.e. $\mathrm{F_{sh}}/\left(\mathrm{F}*+\mathrm{F_{sh}}\right) \simeq 0.43$. No other source in the field seems able to contribute appreciably. The total flux is $\mathrm{F} = 8.55\mathrm{x}10^{-11}\mathrm{Wm}^{-2}$ which corresponds to $\mathrm{m_{bol}} = 6.16$. Adopting the observed parallax or the estimated true parallax, one obtains $\mathrm{M_{bol}} = -1.6^{-2.8}_{-0.85}$ or -3.0 respectively, the true value lying probably close to -2 or -2.5. This calculation confirms that HD 100764 is not a TP-AGB star.

Skinner (1994) used a cylindrical disc in his model. Assuming the star is radiating isotropically and the disc as being isotropic, our result would imply that the disc extends for $\pm 38^\circ$ from its equator, as seen from the star, which is a rather thick disc. This is a lower limit corresponding to a disc optically thick on $76^\circ$. As a consequence, the line of sight has to be within a cone of $52^\circ$ half-angle around the polar axis. This estimate could be perverted if appreciable light is scattered in the disc preferentially towards the observer. Efficient scattering in the IR would however require very large grains which brings us back to the first possibility.

The HC1 stars (i.e. basically early R carbon stars) are low luminosity objects ($\mathrm{M_V} \simeq 0.4$, Vandervort 1958, Gordon 1968, Richer 1975) well below the AGB. Helium flashes in a shell (thermal pulses) thus cannot be the mechanism which generated the shell from HD 100764. If core helium flash in a RGB star could be responsible, we should observe at least a few similar objects. A special model is probably required.

The chemical peculiarities of some low luminosity giants (BaII, CH, extrinsic S stars..) are usually explained in terms of mass transfer or wind accretion in a binary system (McClure et al. 1980, McClure & Woodsworth 1990, Han et al. 1995, Jorissen et al. 1998). The formerly more massive component, now a white dwarf, polluted its companion while a mass loosing TP-AGB star. Dominy (1984) did not find any evidence that HD 100764 might be a binary star and the same situation prevails from HIPPARCOS data (HIC 56551 in ESA 1997). More generally, McClure (1997) found no evidence for binary motion in 16 years of radial-velocity observations of a sample of 22 R-type carbon stars. This is however not a definitive argument against the binary hypothesis but the exceptional nature of HD 100764 would be confirmed in case of detection.

We found large dust temperatures (at least 900 K), wide angular extension and substantial powering of the shell. As proposed by Skinner (1994), the companion wind may have been channeled into a disc (and not onto the surface of HD 100764 which would explain the absence of s-processed elements in the star spectrum). With mass shed through the external Lagrangian point, the disc might be a circumbinary one. Also photocenters deviations were not detected by HIPPARCOS when separation is low and period close to one year (ESA). A much shorter period would result in observable variable velocities. Rather stringent conditions probably restrain the life time of such a configuration which would explain why no other such object is known at present. Finally, the disc geometry might look like the one proposed by Waelkens et al. (1996, their Fig. 2) for HD 44179 (The Red Rectangle), a peculiar A-supergiant orbiting a low-mass object, except that the latter one is viewed nearly edge-on. HD 100764 seen equator-on would mimic a non-variable IRAS C star. This is the reason why we are currently searching for reddened HC stars among them. Unfortunately, short wavelengths data is usually missing.

## 3. The stars with oxygen-type SEDs

### *3.1. Introduction*

A few stars catalogued in Stephenson (1989) are not analysed in terms of the HC and CV-groups we introduced for carbon stars. Their SEDs are typically those of hot stars. Some of them

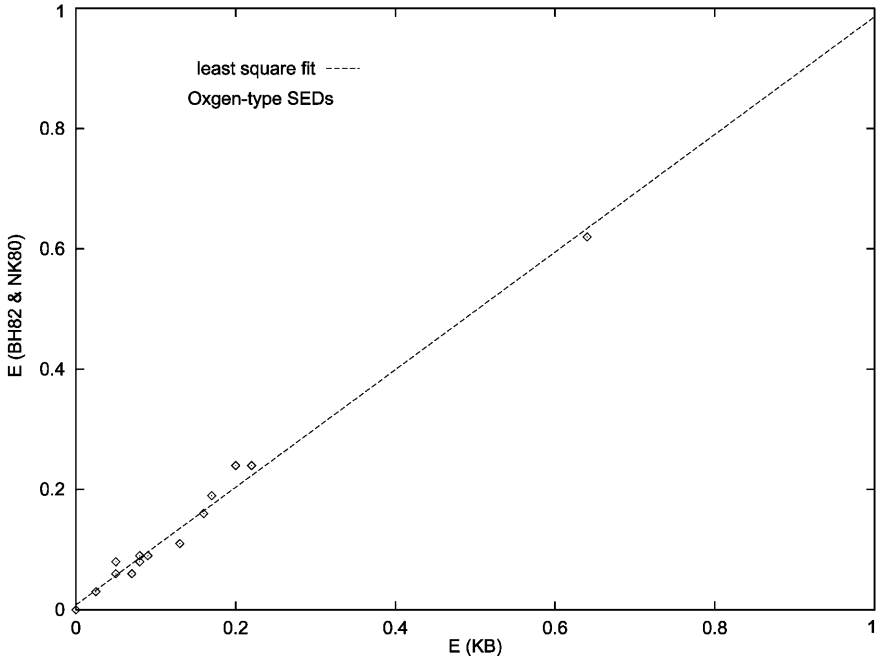


**Fig. 5.** A comparison of E(B-V) excesses from the maps and graphs of Neckel & Klare (1980, NK80) and Burstein & Heiles (1982, BH82) with values from the present paper (KB) for stars with oxygen-type SEDs. The regression line (5) is also shown.

are also Ba II stars. They can be analysed making use of the oxygen-type SEDs we adopted for Ba II stars (Bergeat & Knapik 1997). We have also studied a sample of well-documented RCB stars, the RV Tauri-type carbon star AC Her and V345 Her a carbon Cepheid. The results are given in Table 5. Most of these SEDs can be interpreted with oxygen-type SEDs of giants (g for class III) or supergiants (sg for class Ib). Six RCB stars made exception (1 HC0, 4 HC1 and 1 HC3) which are nevertheless included here. Obviously, they represent the cool end in our sample of RCB stars. The SEDs of hot RCBs are classified F-G while cooler stars in the K- range do have SEDs of the HC-type. This is the well-known junction at G-types, between SEDs of carbon-rich and oxygen-rich stars. The derived oxygen-type group is very often close to the spectral type and luminosity class from spectroscopy. Both may well be variable in a few objects like C 3533 = V553 Cen, a type II-Cepheid (see GCVS). We find again the fact that the SEDs of the hottest carbon-rich stars tend to oxygen-type SEDs. This was already noted by Goldsmith et al. (1987) for carbon-rich yellow supergiants.

### *3.2. The interstellar extinctions*

With the exception of C3982 = RS Tel at minimum light and C4098 = V CrA at an intermediary phase, our values of E(B-V) are found to be close to those from maps in the literature (see Table 5). The former two analyses are discussed in Sect. 3.4. as an illustration of CS extinction. We conclude that the remaining 25 SEDs (22 stars) in Table 5 show, at the corresponding epochs, no selective circumstellar extinction on the line of sight. This is the case of the RCB variables or AC Her then at maximum light. We thus attribute the corresponding colour excess to the interstellar extinction on the line of sight to the star. As mentioned in the notes of Table 5, near IR excesses are however observed. Those near IR excesses, characteristic of dust at an equivalent blackbody temperature of $\sim 900\,\mathrm{K}$, are a general feature of the RCB-class (Feast & Glass 1973). The only possible exception in our Table 5 is $\rho$ Cas. We show in Fig. 5 the plot of the data from the maps in the literature (see Refs. in Sect. 2.3.) against our results. The linear fit obtained for oxygen-types SEDs:

$$\mathrm{E_{NK-BH}} = 0.978\,\mathrm{E_{KB}} + 0.008 \qquad (6)$$

is also shown, with a correlation coefficient of 0.989 (see Eq. 6 of Paper I for a definition). The standard deviation of the slope is 0.026 while it is 0.016 on a single ordinate estimate. The first bisector is thus within the error domain in this diagram, which is quite satisfactory. We attribute to selective CS extinction the extra $\Delta\mathrm{E}\,(\mathrm{B}-\mathrm{V}) = 0.64$ of C 3982 at minimum light and $\Delta\mathrm{E}\,(\mathrm{B}-\mathrm{V}) = 0.11$ of C 4098 at an intermediary phase.

### *3.3. The RV Tauri-type star AC Her*

We have applied our method (see Fig. 6) to the nearly simultaneous data on AC Her (within 40 min..; at JD 2446248,47 i.e. $\Phi$=0.66) published by Goldsmith et al. (1987). A good fit is obtained (G0g, $\mathrm{E}\,(\mathrm{B}-\mathrm{V}) = 0.17 \pm 0.01$, internal error) with six points from U (extreme right) to J leftwards. An increasing IR excess is then observed at H, K and L with respect to the model. This is consistent with the analysis of Goldsmith et al. as shown by their Fig. 2b. The excess is still larger in the IRAS-bandpasses (for instance 6.3 mag at [12] and 8.1 mag at [25]; the IRAS Point Source Catalogue 1988; AC Her = IRAS 18281+2149). The silicate emission at 10 $\mu$m and 18 $\mu$m is obvious in its LRS Spectrum. Due to the scale of Fig. 6 the corresponding points cannot be displayed: the stellar photons are outnumbered by circumstellar photons. The field interstellar colour excess is found to be less or equal to 0.19–0.21 from the published maps (see Refs. in Sect. 2.2.), while Goldsmith et al. quoted $\mathrm{E}\,(\mathrm{B}-\mathrm{V}) = 0.10$

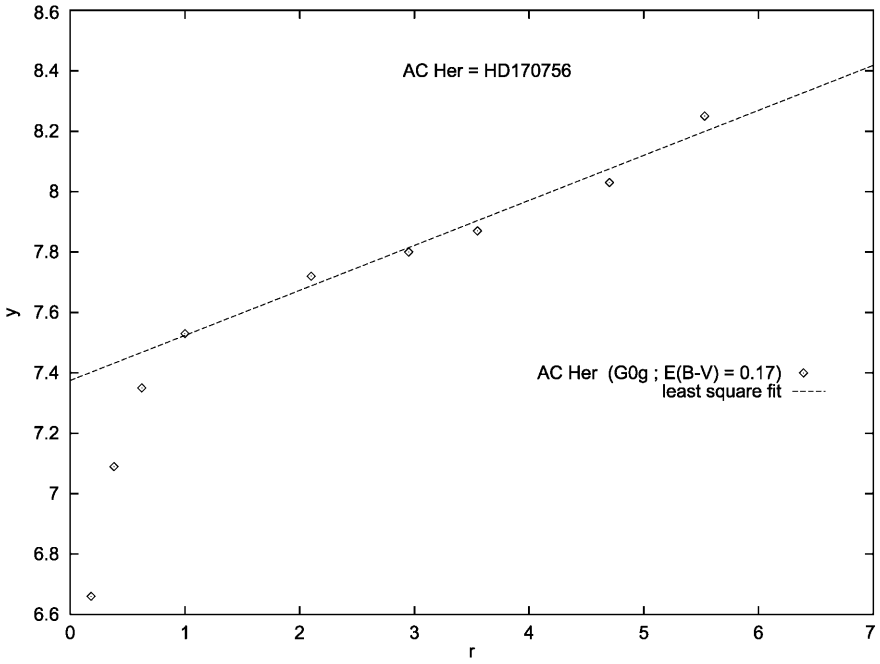


**Fig. 6.** The plot of y *vs.* r illustrating Eqs. (1) and (2) in the case of AC Her (G0g, E(B-V) = 0.17). The slope is A(J) the extinction at $\lambda = 1.25\,\mu\mathrm{m}$ and the intercept is $V_0$ the dereddened magnitude at $0.55\,\mu\mathrm{m}$. The IR excess starts from r=0.62 (H-filter). See Sect. 3.3. for details.

in their Table 3. Clearly no room is left for a substantial contribution of selective CS extinction on the line of sight (Goldsmith et al. concluded to $\mathrm{E\,(B-V)_{CS}} = 0.04$ which appears here as an upper limit). Concerning the CS extinction, we are left with the same two possible conclusions as in Sect. 2.4., viz.:

- it is essentially wavelength-independent at least up to $\lambda_{\mathrm{J}}$ = 1.25 $\mu\mathrm{m}$ which points to large grains (radii $\mathrm{a} \simeq 0.3\,\mu\mathrm{m}$ or even larger),
- and/or it is strongly non-spherical in distribution (e.g. a disc or torus seen at a large inclination angle nearly pole on) or even patchy.

As we did for HD 100764, we favour the second hypothesis. Since AC Her is a RV Tau-a star, i.e. it has a constant mean light, we suggest that no CS dust is present on the lines of sight to those stars. Conversely, intervening CS dust on the line of sight of a RV Tau-b star would be responsible for their redder colours and cyclical variations of mean lights. It is plausible that mass loss proceeds more or less sporadically in RV Tau stars (Lloyd Evans 1985, Goldsmith et al. 1987). Recently Van Winckel et al. (1998) have confirmed that AC Her is in fact member of a wide binary system. These authors favour the existence of a long-lived disc in the system, the gas-dust separation accounting for the depletion pattern of refractory elements.

Finally, we briefly discuss the type of the adopted SED, i.e. G0g. Apart from Rp and C0,0 classifications, the quoted spectral types from various catalogues available at CDS are F2pIb-K4e, F4IbP var, and F8. The nearest of our photometric groups should be F5sg, F8sg and G0sg. They yield solutions ranging from less good (F5sg) to very bad (F8sg and G0sg). The observed HIPPARCOS parallax of $(0.7 \pm 1.09)\,\mathrm{mas}$ seems to preclude the class III but not the class II, and of course also Ib. We have tried to exploit some additional non-simultaneous SEDs. The solutions ranged from G0g, E(B-V)=0.14 to F8sg, E(B-V)=0.3, but none was as good as the one adopted above (G0g, E(B-V)=0.17). Clearly, we need more simultaneous data obtained on the whole spectral range at various phases.

### *3.4. The R Coronae Borealis variables*

#### 3.4.1. Introduction

We display in Fig. 7 the diagram of y *vs.* r for R CrB, the prototype of its class. The solution is F8sg, E(B-V)=0.0. For the same reasons we mentioned in Sect. 2.4., we favour the absence of both interstellar and circumstellar extinctions on the line of sight, at the time of the observations. Large IR excesses are seen which can be attributed to dust outside the line of sight. The RCB-stars are evolved variable objects (usually hydrogen-poor and carbon-rich) often classified as F-G supergiants. They show large amplitude variations with deep minimas attributed to strong extinction on the line of sight (e.g. Feast et al. 1997 and references therein). It was shown from simple geometrical considerations that the dust condensates close to the star in patchy puffs. Then clearing occurs while they expand and/or leave the line of sight. The calculated dust temperatures (3000 K in the vicinity of a 6000 K star) are however by far too high for known species to condense and survive. Following Goeres & Sedlmayr (1992), the condensation temperature depends on the local density in a range of 1200 K to 1600 K which is reached at distances larger than 10 stellar radii in standard models of pulsating atmospheres. However, dust formed at 20 stellar radii cannot explain the fast recovery times because the dissipation time is too long (e.g. Clayton, 1996). Woitke et al. (1996) have studied the thermal balance, chemistry and nucleation in fluid elements of CS envelopes around RCB stars, periodically hit by strong shock waves due to pulsation (periods of 40–50 days).

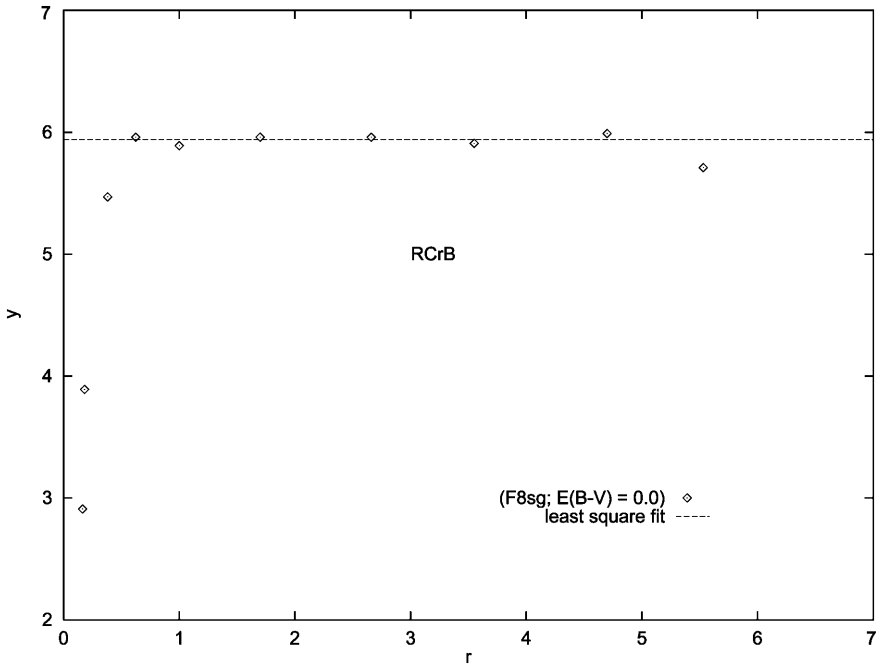


**Fig. 7.** Same as Fig. 6 for R CrB: strong IR excesses are noted for $r \leq 0.38$ (K-filter and beyond) when compared to the extrapolated dashed line.

Non-LTE radiative heating and cooling via various processes are taken into account. After compression and heating, the element radiates and re-expands with adiabatic cooling. Abundant polar molecules (like possibly the carbon monoxide CO) should play a substantial role in the cooling process. Gas temperatures lower than estimated from radiative equilibrium are reached, e.g. 1500 K at 1.5 to 3 stellar radii (Woitke et al. 1996). Carbon dust can form from chains or clusters, in "puffs" then ejected by radiation pressure. The conditions might still be improved in puffs formed above giant convective cells (Wdowiak 1975). As noted by Feast (1997), it is not clear however whether all RCB stars undergo significant pulsation or whether optical variability outside obscuration minimas occurs which could be attributed to randomly occurring convective cells.

The optical properties and temperatures of the grains depend on their nature. Zubko (1997) analysed the extinction curves available for some RCB stars, making use of the method of regularization for solution of ill-posed problems. The best solutions were obtained making use of graphite with a $0.02$–$0.07\,\mu\mathrm{m}$ size distribution, similar in separate forming clouds. The calculated extinction law is selective. A similar range of glassy or amorphous carbon particles $0.005$–$0.06\,\mu\mathrm{m}$ was already deduced by Hecht et al. (1984), the graphite bump at $\lambda \simeq 0.217\,\mu\mathrm{m}$ being absent from RCB spectra. They concluded to the possibility of larger particles forming initially, and being replaced gradually by a broad distribution of smaller grains. The mechanism could be particle collisions producing a MRN type distribution in a red giant outflow as proposed by Biermann & Harwit (1980).

### 3.4.2. Analyses of variations in two RCB stars

The main results and data we obtained for RCB variables can be found in Sect. 3 and Table 5. Two stars are considered hereafter which we found documented at two epochs, namely V CrA and RS Tel. We present the two studied SEDs of V CrA in Fig. 8. The solution F9g with E(B-V)=0.13 is derived at maximum light (JD 2447390). This colour excess being consistent with maps values, we consider this is the amount of interstellar extinction on the line of sight. The other solution F9g and E(B-V)=0.23 is obtained at JD 2446597.5, on a rising branch of the light curve. The extra $\Delta \mathrm{E}\,(\mathrm{B}-\mathrm{V}) \simeq 0.10$ is attributed to CS dust, no difference between the CS and interstellar laws being detected at the wavelengths we used. We also note that the dereddened magnitudes in Fig. 8 are $\mathrm{V}_0 \simeq 9.50 \pm 0.01$ and $\mathrm{V}_0 \simeq 9.59 \pm 0.05$ respectively, i.e. practically the same value within the internal errors. This is consistent with extinction on the line of sight being responsible of the variations, the star variations remaining negligible. Small grains are indicated here with a selective law similar to the one for the interstellar extinction.

The situation appears as different in deep minimas where a contribution of neutral extinction by large grains seems required. For C 3982 = RS Tel, we have obtained G0sg and E(B-V)=0.07 (interstellar value) at JD 2445217 where V=9.91 was adopted (close to maximum), and G0sg and E(B-V)=0.71 at JD 2445544 deep in a minimum where V=15.05 was adopted (see Fig. 9). The extra $\Delta \mathrm{E}\,(\mathrm{B}-\mathrm{V}) \simeq 0.64$ obtained is CS in origin. The dereddened magnitudes are $\mathrm{V}_0 = 9.74 \pm 0.03$ and $12.89 \pm 0.08$ respectively which could imply more than 3 mags of neutral extinction in addition to the selective component (both contributions would equalize in the UV-blue part of the spectrum). The intrinsic star variations probably amount to a few tenths of a magnitude. This result is suggestive of rapid grain growth in forming dense puffs, followed by destructive collisions then leading to much smaller (selective) grains during clearing. Our results in Table 5 are thus consistent with the analysis of Hecht et al. (1984) and Zubko (1997), with the following conclusions:

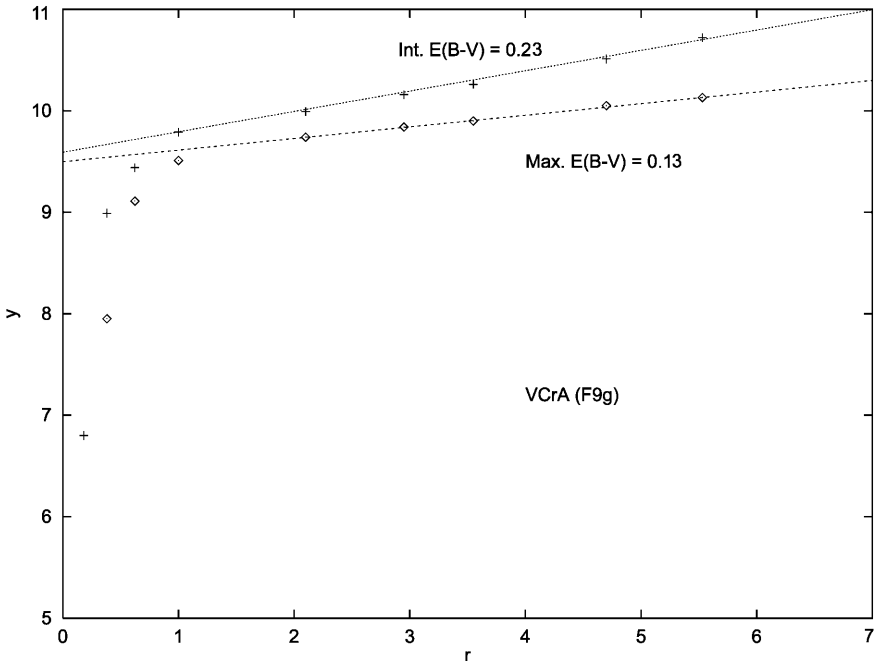


**Fig. 8.** Same as Fig. 6 for V CrA: strong IR excesses are found for $r \leq 0.62$ (H-filter and beyond) when compared to the extrapolated dashed lines. See text for details.

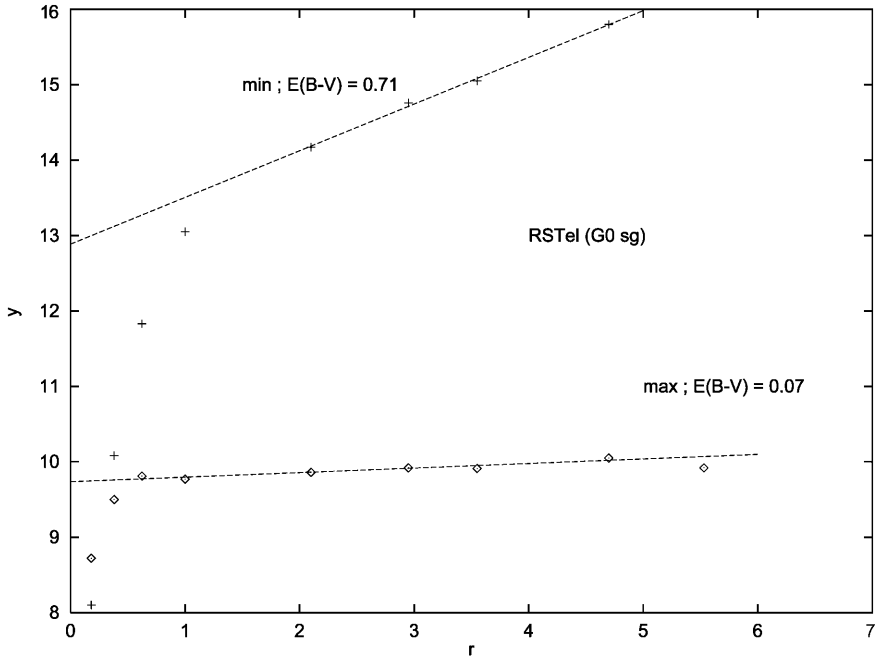


**Fig. 9.** Same as Fig. 6 for RS Tel: strong IR excesses are found from the K or J-filter when compared to the extrapolated dashed lines. See text for details.

– the bright RCB stars studied here at the observed maximas (either oxygen or carbon-type SEDs) have no appreciable CS dust extinction on the line of sight, the observed extinction being interstellar in origin when present,
– relatively small grains are observed which generate a selective circumstellar law not too far from the adopted law for interstellar extinction, except at deep minima where large grains and additional neutral extinction are required for dense puffs,
– the same photometric group is deduced for a given star at various phases consistent with the idea that the variations are essentially non-stellar (see however Rao & Lambert 1997 who find from spectral analysis a difference of 500 K between the maximas and minimas of R CrB); additional data on more stars is needed.

## 4. Discussion and conclusion

The HC stars (Sect. 2) have been classified into six groups (HC0 to HC5) and for those stars, Tables 1 and 2 correspond to their counterparts for CV stars in Paper I. Many of them (about 75%) are non variable stars to the accuracy of presently available measurements (including the HIPPARCOS Hp-data from ESA). They parallel the G0 to M3 sequence of oxygen-rich giants (see

**Table 5.** Stars with oxygen-type SEDs and HC-groups including RCB variables. Their C-entries from Stephenson (1989), or number in the HD-catalogue, or variable star name in the GCVS, are given. The spectral types, peculiarities and variability types are collected in column 2. Our SED-group and colour excess are given in column 3, while the values from maps can be found in column 4 together with additional information such as alternative name or spectral classification; also quoted, the occurrence of an infrared excess relative to our solution from a specified filter (J, H, K..) or not (no).

| Name | SP. TYPE | G, $E_{B-V}$ | $E'_{B-V}$, NOTES |
|---|---|---|---|
| 26 | G4V:p CHBaII | G4g 0.07 | 0.06 C0,0 no |
| C984 | K1K2III BaII | K1g 0.05 | 0.08 no |
| 46407 | G9III BaII | G8g 0.00 | 0.00 no |
| 76115 | K0 CH: | G8g 0.03 | 0.03 |
| 201626 | G9p CH | K0g 0.05 | 0.06 no |
| 121447 | K4III: BaII | K5g 0.05 | 0.06 IT Vir K7 |
| XX Cam | G1Iab:e RCB: | F8sg 0.16 | 0.16 (L) |
| SU Tau | G01Ie HdRCB | F5sg 0.64 | 0.62 (K) |
| RU Aqr | M5IIIe SRb | M6g 0.00 | 0.00 C6,3 no |
| C3533 | G5IIp Cep TII | F8g 0.08 | 0.08 V553Cen |
| C3533 | G5IIp Cep TII | G1g 0.08 | 0.08 V553Cen |
| AC Her | F4Ibpvar RVa | G0g 0.17 | 0.19 (H) |
| R CrB | F8G0Iab RCB | F8sg 0.00 | 0.00 Hd (K) |
| C3982 | R0,C max RCB | G0sg 0.07 | 0.09 RSTel (L) |
| C3982 | R0,C min RCB | G0sg 0.71 | 0.09 RSTel (J) |
| AC Her | F4Ibpv 0.66 RVa | G0g 0.17 | 0.19 (H) |
| C4098 | R0,C max RCB | F9g 0.13 | 0.11 VCrA (J) |
| C4098 | R0,C int RCB | F9g 0.23 | 0.11 VCrA (H) |
| RY Sgr | GOIaep HdRCB | F5sg 0.09 | 0.09 C1,0 (K) |
| $\rho$ Cas | G2IaeSRdRCB: | G4g 0.22 | 0.24 max no |
| $\rho$ Cas | G2IaeSRdRCB: | G8g 0.20 | 0.24 int no |
| C3562 | R3 HdRCB | HC1 0.23 | 0.24 S Aps (K) |
| C3687 | R HdRCB | HC0 0.32 | 0.30 RT Nor (K) |
| C3950 | R5 HdRCB | HC1 0.18 | 0.15 WX CrA (K) |
| C3999 | R0 HdRCB | HC1 0.11 | 0.15 GU Sgr (K) |
| C4181 | R2R5 HdRCB | HC3 0.46 | 0.36 SV Sge (L) |
| C5549 | R HdRCB | HC1 0.00 | 0.00 U Aqr (L) |

Table 2). The difference between "carbon" and "oxygen" SEDs continuously diminishes when dealing with earlier groups or spectral types, and it finally vanishes at type G. The SEDs of RCB stars and others (AC Her as a RV Tau star and a few BaII or HdC stars) were found to belong to the oxygen-rich category (see Sect. 3 and Table 5). The stars described in this paper span the 3300–7500 K range in effective temperatures.

While of less accuracy when compared to Paper I study, the evaluation of the interstellar extinction on HC stars is quite acceptable (Sect. 2.3.) It proves excellent for oxygen-types SEDs (Sect. 3.2.). The results for about 140 stars are provided in Tables 3 and 4 on a single homogeneous scale which is found compatible with those from other methods. The comparison between the derived excesses and those obtained from maps in the literature has proved satisfactory.

We have been able to disentangle the circumstellar and interstellar extinctions in a few cases and some conclusions are reached about the CS grains and their spatial distribution. A disc model with carbon grains is favoured for the exceptional HC1 star HD 100764, as proposed by Skinner (1994). It appears however as a very thick one subtending at least a total angle of $76^\circ$ with 43% of the observed luminosity being from the shell. The interstellar extinction found for the carbon-rich RV Tau-a star AC Her is found to be E(B-V)=0.17 with a G0g classification. No CS extinction on the line of sight is detected. It could be a common feature of the "constant mean light" RV Tau-a stars. Variable CS extinction on the line of sight to RV Tau-b stars would be the rule as suggested by redder colours and fluctuating mean light.

Finally, we have determined the groups and extinctions for a sample of RCB stars. The interstellar component is given in Table 5, as derived from observations at maximum light. Two stars (V CrA and RS Tel) were studied while obscured. Large (neutral) carbonaceous grains substantially contribute to dense puffs during deep minimas while distributions peaking towards smaller (selective) grains are predominant after some clearing, before maximum light. Those features can be explained in terms of destructive collisions in expanding puffs. Such collisions are the mechanism suggested by Biermann & Harwit (1980) to generate the $a^{-3.5}$ radii distribution (MRN) used in the classical models of the interstellar extinction law.

*Acknowledgements.* Valuable suggestions from the referee Dr. J.M. Winters are gratefully acknowledged.

## References

Baumert J.H., 1972, unpublished thesis, The Ohio State University
Bergeat J., Knapik A., 1997, A&A 321, L9
Bergeat J., Knapik A., 1998, to be submitted to A&A
Bessell M.S., 1979, PASP 91, 889
Bessell M.S., Brett J.M., 1988, PASP 100, 1134
Biermann P., Harwit M., 1980, ApJ 241, L105
Burstein D., Heiles C., 1982, AJ 87, 1165
Catchpole R.M., Feast M.W., 1971, MNRAS 154, 197
Chan S.J., 1994, MNRAS 268, 113
Clayton G.C., 1996, PASP 108, 225
de Jong T., 1989, A&A 223, L23
Dominy J.F., 1984, ApJS 55, 27
Dominy J.F., Lambert D.L., Gehrz R.D., Mozurkewich D., 1986, AJ 91, 951
ESA, 1997, The HIPPARCOS Catalogue. ESA SP-1200 (ESA)
Feast M.W., 1997, MNRAS 285, 339
Feast M.W., Glass I.S., 1973, MNRAS 161, 293
Feast M.W., Carter B.S., Roberts G., Marang F., Catchpole R.M., 1997, MNRAS 285, 317
FitzGerald M.P., 1968, AJ 73, 983
Goeres A., Sedlmayr E., 1992, A&A 265, 216
Goldsmith M.J., Evans A., Albinson J.S., Bode M.F., 1987, MNRAS 227, 143
Gordon C.P., 1968, ApJ 153, 915
Han Z., Eggleton P.P., Podsiadlowski P., Tout C.A., 1995, MNRAS 277, 1443
Hecht J.H., Holm A.V., Donn B., Wu C.C., 1984, ApJ 280, 228
IRAS Science Team 1986, A&AS 65, 607 (LRS)

IRAS Point Source Catalog, version 2, 1988, Joint IRAS Science Working Group, 3. vols. 1–6, NASA RP-1190, Washington D.C.: U.S. Government Printing Office
Johnson H.L., 1966, ARA&A 4, 193
Johnson H.L., McArthur J.W., Mitchell R.I., 1968, ApJ 152, 465
Jorissen A., Van Eck, S., Mayor M., Udry S., 1998, A&A 332, 877
Keenan P.C., 1993, PASP 105, 905
Keenan P.C., Morgan W.W., 1941, ApJ 94, 501
Kholopov P.N., Samus N.N., Frolov M.S., et al., 1985 General Catalogue of Variable Stars. Nauka Publishing House, Moscow (GCVS). Suppl. Lists 67 (1985, IBVS 2681), 68 (1987, IBVS 3058), 69 (1989, IBVS 3323), 70 (1990, IBVS 3530), 71 (1993, IBVS 3840), 72 (1995, IBVS 4140) & 73 (1997, IBVS 4471)
Knapik A., Bergeat J., 1997, A&A 321, 236 (Paper I)
Knapik A., Bergeat J., Rutily B., 1998, A&A 334, 545
Koornneef J., 1983, A&A 128, 84
Kukarkin B.V., Kholopov P.N., Artiukhina N.M., et al., 1982, New Catalogue of Suspected Variable Stars. Nauka Publishing House, Moscow (NSV).
Little-Marenin I.R., 1986, ApJ 307, L15
Lloyd Evans T., 1985, MNRAS 217, 493
McClure R.D., 1997, PASP 109, 256
McClure R.D., Fletcher J.M., Nemec J.M., 1980, ApJ 238, L35
McClure R.D., Woodsworth A.W., 1990, ApJ 352, 709
Mathis J.S., 1990, ARA&A 28, 37
Mendoza E.E.V., 1968, Pub. Dept. Astron. Univ. Chile 1, No 7, p. 106
Neckel T., Klare G., 1980, A&AS 42, 251
Parthasarathy M., 1991, MNRAS 247, 429
Rao N.K., Lambert D.L., 1997, MNRAS 284, 489
Richer H.B., 1975, ApJ 197, 611
Shane C.D., 1928, Lick Obs. Bull. 13, 123
Skinner C.J., 1994, MNRAS 271, 300
Stephenson C.B., 1989, Pub. of the Warner & Swasey Obs. 3, No. 2
Van Winckel H., Waelkens C., Waters L.B.F.M., et al., 1998, A&A 336, L17
Vandervort G.L., 1958, AJ 63, 477
Waelkens C., Waters R., Van Winckel H., 1996, In: Science with the VLT Interferometer. Proc. ESO Workshop 18–21/06/96, Springer
Wdowiak T.J., 1975, ApJ 198, L139
Willems F.J., de Jong T., 1986, ApJ 309, L39
Woitke P., Goeres A., Sedlmayr E., 1996, A&A 313, 217
Zubko V.G., 1997, MNRAS 289, 305